

Targeting PI3K/Akt/mTOR Pathway Identifies Differential Expression and Functional Role of IL8 in Liver Cancer Stem Cell Enrichment



Deniz Cansen Kahraman¹, Tamer Kahraman², and Rengul Cetin-Atalay¹

Abstract

Activation of the PI3K/Akt/mTOR pathway is an important signaling mechanism involved in the development and the progression of liver cancer stem cell (LCSC) population during acquired Sorafenib resistance in advanced hepatocellular carcinoma (HCC). Therefore, identification of novel therapeutic targets involving this pathway and acting on LCSCs is highly essential. Here, we analyzed the bioactivities and the molecular pathways involved in the action of small-molecule PI3K/Akt/mTOR pathway inhibitors in comparison with Sorafenib, DNA intercalators, and DAPT (CSC inhibitor) on CD133/EpCAM-positive LCSCs. Sorafenib and DNA intercalators lead to the enrichment of LCSCs, whereas Rapamycin and DAPT significantly reduced CD133/EpCAM positivity. Sequential treatment with Rapamycin followed by Sorafenib decreased the ratio of LCSCs as well as their sphere formation capacity, as opposed to Sorafenib alone. Under the stress of the inhibitors,

differential expression analysis of 770 cancer pathway genes using network-based systems biology approach singled out *IL8* expression association with LCSCs. Furthermore, *IL8* secretion and LCSC enrichment ratio was also positively correlated. Following *IL8* inhibition with its receptor inhibitor Reparixin or siRNA knockdown, LCSC features of HCC cells were repressed, and sensitivity of cells to Sorafenib increased significantly. Furthermore, inflammatory cytokines (*IL8*, *IL1 β* , and *IL11*) were also upregulated upon treatment with HCC-approved kinase inhibitors Sorafenib and Regorafenib. Hence, chemotherapeutic stress alters inflammatory cytokine gene expression in favor of hepatic CSC population survival. Autocrine *IL8* signaling is identified as a critical event, and its inhibition provides a promising complementary therapeutic approach for the prevention of LCSC population enrichment.

Introduction

Hepatocellular carcinoma (HCC) has become a major global burden due to significantly increased incidence in the world; it constitutes 7% of cancer deaths and is one of the leading cause of cancer mortality globally (1). In the United States, liver cancer death rates increased 43% between 2000 and 2016 (2). Increased life expectancy and growth in old age population across developed countries have also affected cancer types previously not accounted for (3). Injured hepatocytes due to various etiologic factors (viral, alcohol abuse, toxins, obesity, and metabolic syndrome) initiate chronic inflammatory disease state which involves death and regeneration cycles of hepatocytes leading to cirrhosis and eventually to the progression toward HCC (4). In this process, hepatic progenitor cells (HPC) are damaged and

transformed to liver cancer stem cells (LCSC) which are responsible for chemoresistance, tumor relapse, and metastasis (5). Sorafenib and Regorafenib are multikinase inhibitors, which are used for the treatment of advanced HCC patients. However, HCC patients acquire frequent resistance to Sorafenib (3). The underlying mechanisms of this resistance yet to be solved involve crosstalk of PI3K/Akt and JAK-STAT pathways, epithelial-mesenchymal transition events, leading to the enrichment of LCSCs (6). Therefore, identification of protein targets involved in the enrichment of LCSCs will be essential for the development of novel therapeutic approaches for HCC. The PI3K/Akt/mTOR pathway is one of the most critical pathways involved in the development and progression of many cancer types including HCC (7). Under normal circumstances, the activity of this pathway is under the control of tumor-suppressor protein PTEN. However, anomalies in PTEN function are commonly observed in HCC leading to the hyperactivation of PI3K/Akt/mTOR pathway (8). In addition, this pathway is involved in crosstalk with the JAK-STAT and MAPK pathways upon treatment with Sorafenib, which has been considered as one of the mechanisms associated with acquired Sorafenib resistance in HCC (9). Therefore, targeting the PI3K/Akt/mTOR pathway with various inhibitors has been highlighted for its therapeutic potential in combination with Sorafenib. Inflammation in chronic liver disease and cancer plays a vital role in differentiation and proliferation of HPCs. During this transformation, hepatocytes activate the resident immune cells that result in release of cytokines and chemokines into the microenvironment to recruit immune cells (10). These events cause hepatic regeneration and tumor progression to take place

¹Cancer Systems Biology Laboratory, Graduate School of Informatics, ODTU, Ankara, Turkey. ²Department of Molecular Biology and Genetics, Bilkent University, Ankara, Turkey.

Note: Supplementary data for this article are available at Molecular Cancer Therapeutics Online (<http://mct.aacrjournals.org/>).

Corresponding Author: Deniz Cansen Kahraman, Cancer Systems Biology Laboratory, Middle East Technical University, Universiteler Mah. Dumlupinar Blv, No:1 ODTU Ankara, Ankara 06800, Turkey. Phone: 90-312-210-7374; Fax: 90-312-210-3745; E-mail: cansen@metu.edu.tr

Mol Cancer Ther 2019;18:2146-57

doi: 10.1158/1535-7163.MCT-19-0004

©2019 American Association for Cancer Research.

leading to HCC. Serum cytokine levels in HCC patients have been associated with poor prognosis and aggressive behavior of cancer cells and induce cancer stem cell-like properties (11).

Here, we report that LCSC population in HCC cell lines is affected differentially by different PI3K/Akt/mTOR pathway inhibitors, where mTOR inhibitor Rapamycin was found to inhibit the enrichment of LCSCs and suppress the upregulation of *IL8* triggered by Sorafenib. Our results also revealed *IL8* as a potential target for CSCs, where *IL8* blockade or downregulation prevented enrichment of LCSCs significantly.

Experimental Procedure

Detailed experimental procedures were given in Supplementary documentation.

Cell culture

HCC cell lines were obtained from the following resources: Hep3B (ATCC-HB-8064), SNU475 (ATCC-CRL-2236), Huh7 (ATCC-JCRB0403), and Mahlavu (12). All cell lines used in this study are short tandem repeat authenticated, and contamination with mycoplasma was regularly tested with mycoplasma test kit (MycoAlert, Lonza). The passaging of the cells was minimized throughout the experiments (two times a week, maximum 8–10 passages). Huh7, Hep3B, and Mahlavu cells were maintained in DMEM (Invitrogen GIBCO), supplemented with 10% FBS (Invitrogen GIBCO), and 0.1 mmol/L nonessential amino acid, whereas SNU475 cells were maintained in RPMI (Invitrogen GIBCO), supplemented 10% FBS and 2 mmol/L L-glutamine. Cells were grown in a humidified incubator at 37°C and 5% CO₂ with mediums containing 100 units/mL penicillin and streptomycin.

Flow cytometry and isolation of side populations

Cells were fixed with 4% paraformaldehyde for 20 minutes and stained with anti-CD133/1 (AC133)-Biotin, anti-biotin-PE, anti-EpCAM-FITC, or anti-CD90-FITC antibodies according to the manufacturer's protocol (Miltenyi). For stemness protein detection, cells were permeabilized with 90% ice-cold methanol 10 minutes prior to blocking, and NANOG and OCT4 antibodies, and anti-rabbit IgG-Alexa 647 were used for staining. Analyses were done using BD Accuri C6 Flow Cytometer (BD Biosciences) or Novocyte flow cytometer (ACEA Biosciences). CD133, EpCAM-positive, and -negative cells were sorted with FACSMelody Cell Sorter (BD Biosciences), and their purity was assessed using flow cytometry.

Sulforhodamine B cytotoxicity assay

Cells were inoculated into 96-well plates (1,000–2,000 cells/well). After 24 hours, cells were treated with the inhibitors and DMSO control in 40 to 0.1 μmol/L concentrations. Cells were fixed after 72 hours by cold 10% (w/v) trichloroacetic acid (MERCK) for an hour. Cells were washed 3 times with ddH₂O and then 50 μL of 0.4% sulforhodamine B (SRB) dye (Sigma-Aldrich) was applied to each well and incubated at room temperature for 10 minutes. Wells were washed with 1% acetic acid for 4 times and left for air-drying. SRB dye was solubilized in 100 μL/well 10 mmol/L Tris-Base solution, and absorbance was measured at 515 nm (ELx800, BioTek).

Sphere formation

Cells formed spheres in ultralow attachment 96-well plates for 6 to 12 days containing DMEM/F12 serum-free medium (Gibco,

Invitrogen) supplemented with EGF (20 ng/mL; Thermo Fisher), basic fibroblast growth factor (10 ng/mL; Sigma), B27 supplement (1:50; Invitrogen), Heparin (2 μg/mL; Sigma), insulin (5 μg/mL; Sigma), hydrocortisone (0.5 μg/mL; Sigma), and 100 units/mL penicillin and streptomycin (Gibco, Invitrogen).

Analysis of gene expression

Huh7 cells were treated with the optimum mutual inhibitory concentration (OMIC) values of the inhibitors and DMSO controls for 72 hours, then total RNA was extracted (RNeasy Mini Kit Qiagen), and nCounter PanCancer Panel gene expression analysis was performed as instructed by the manufacturer. Quality control, normalization, and differential expression analysis were done with nSolver 3.0.

Cellular pathway analysis

Differential expression values (Supplementary Tables S1 and S2) were ranked, and the lists were uploaded to Cytoscape 3.5 software platform and analyzed with the pathway scoring application on "Pathways in cancer (hsa05200)" KEGG pathway. The enrichment scores assigned by the algorithm reflect the biological response of a specific process in the pathway.

siRNA transfection

Three different *IL8* siRNAs (Hs_IL8_6 FlexiTube siRNA_validated, Hs_IL8_5 FlexiTube siRNA_validated, and Hs_IL8_4 FlexiTube siRNA) were purchased from Qiagen (Qiagen Inc.). Hs_IL8_6 FlexiTube siRNA was used for *IL8* knockdown. Cells were seeded onto 6-well plates (105 cells/well). After 24 hours, at 50% to 70% confluency, cells were treated with Hs_IL8_6 FlexiTube siRNA_validated (50 nmol/L) or negative control siRNA (si-neg) using HiPerFect transfection reagent according to the manufacturer's instructions. Media were replaced with 10% complete DMEM after 16 hours, and cells were collected after 24, 48, or 72 hours for further experiments.

Quantitative RT-PCR

RevertAid First Strand cDNA synthesis kit (Thermo Scientific) was used for cDNA synthesis from Total RNA. Quantitative PCR was performed using Light Cycler 96 Real-Time PCR System with LightCycler 480 SYBR Green I Master (Roche). The experimental Ct (cycle threshold) was calibrated against GAPDH. The $\Delta\Delta C_t$ method was used to determine the amount of target gene in inhibitor treated cells relative to DMSO-treated cells.

ELISA

Anti-human *IL8* ELISA studies were conducted using Nunc MaxiSorp ELISA plates (Millipore Sigma) and human *IL8* (CXCL8) ELISA development kit (Mabtech, Sweden) as recommended by the manufacturer. Optical density values were detected on an ELISA reader (Spectramax, Molecular Devices) at 405 nm.

Western blot analysis

Protein electrophoresis (Mini-PROTEAN Tetra Cell Systems and TGX precast gels) and transfer system (Trans-Blot Turbo Transfer System) were used according to the manufacturer's protocol for Western blot analysis. Proteins were transferred to a PVDF-LF membrane and visualized using C-Digit or Odyssey Clx imaging system (LI-COR) after incubation with primary and secondary antibodies (provided in Supplementary Information).

Real-time cell growth monitoring

Huh7 cells were inoculated into 16-well E-plates (8,000 cell/well). After 16 hours, cells were either transfected with *IL8* siRNA (experimental group) or left inside culture media (control group) for 16 hours. Then, cells were treated with Sorafenib to be monitored for at least 96 hours by real-time cell electronic sensing system (RT-CES), xCELLigence SP system (ACEA Biosciences), as recommended by the manufacturer. Cell index values were used to plot growth curves of cells.

Statistical analysis

All data in this study were obtained from three independent experiments and $n \geq 3$ biological replicates. Statistical analysis was performed using a Student *t* test (Prism, Graphpad, or Microsoft Excel). Mean fluorescence intensity values of all flow cytometry analysis results were provided in Supplementary Fig. S11. Statistically significant results were represented as follows: *, $P < 0.05$; **, $P < 0.01$; and ***, $P < 0.001$.

Results

PI3K/Akt/mTOR pathway inhibitors display differential effects on CD133⁺/EpCAM⁺ LCSC population

We recently reported that CD133 and EpCAM were suitable to detect LCSCs of epithelial-like cells, whereas CD90 was efficient to detect LCSCs of mesenchymal-like cells (13, 14). CD133⁺/EpCAM⁺ and CD133⁻/EpCAM⁻ populations from Huh7 and Hep3B cells were separated by cell sorter with a purity and sorting efficiency of approximately 95% (Supplementary Fig. S1A). To characterize stemness features of the isolated cells, sphere formation and stemness factors' (NANOG and OCT4) expression were compared in CD133⁺/EpCAM⁺ and CD133⁻/EpCAM⁻ populations. CD133⁺/EpCAM⁺ cells were able to form vivid and dense spheres, whereas CD133⁻/EpCAM⁻ cells were unable to form such spheres (Supplementary Fig. S1B). In addition, NANOG and OCT4 expressions were higher in CD133⁺/EpCAM⁺ cells (Supplementary Fig. S1C). Thus, these markers were suitable for studying cells that have LCSC characters.

Moreover, the activity of the PI3K/Akt/mTOR pathway was analyzed in the presence of Sorafenib (Selleck chemicals) in Huh7 and Mahlavu cells. After 72 hours of treatment with Sorafenib, the PI3K/Akt/mTOR pathway proteins were shown to remain active (Supplementary Fig. S2), which supported the findings reported in previous studies (6, 9).

Ten PI3K/Akt/mTOR pathway inhibitors, DNA intercalators [Camptothecin (15; MERCK), and Doxorubicin (16; SABA)], and Sorafenib were used to determine their effects on LCSCs. Initially, the inhibitory concentrations of these inhibitors on HCC cells (Huh7, Hep3B, Mahlavu, and SNU475) were identified. The IC₅₀ values showed small differences between cell lines; therefore, an OMIC value was set for all the inhibitors targeting HCC cells throughout the following experiments in this study (Supplementary Fig. S3A).

To observe the changes in the expression of stem cell markers with each inhibitor, cells were treated for 72 hours with their OMIC values and compared with DMSO controls. Treatment of HCC cells with Sorafenib and DNA intercalators enriched the CD133⁺/EpCAM⁺ cells. PI3K/Akt pathway inhibitors led either to the enrichment of CD133⁺/EpCAM⁺ cells [ZSTK474 (17), NVP-BEZ235 (18)] or did not have any effect [Akti-1,2 (19), Akti-2 (20), PI3Ki- α (21), PI3Ki- β (22)]. However, mTOR

inhibitor-Rapamycin (ref. 23; Calbiochem), PI3K inhibitor-LY294002 (ref. 24; Calbiochem), and Notch inhibitor-DAPT (ref. 25; Selleck chemicals) significantly reduced the CD133⁺/EpCAM⁺ cells (Fig. 1; Supplementary Fig. S3B). Yet, because LY294002 displayed its effect in lower significance, Rapamycin was selected for combination experiments with Sorafenib.

Moreover, Sorafenib and Doxorubicin significantly increased CD90 positivity in mesenchymal-like HCC cells (Mahlavu and SNU475), whereas Rapamycin and DAPT decreased the amount of CD90-positive cells (Supplementary Fig. S4). Hence, rapamycin was able to prevent enrichment of CSCs in both epithelial- and mesenchymal-like HCC cells similar to the effect of DAPT.

Rapamycin treatment prior to Sorafenib prevents LCSC enrichment

Recent studies indicate that mTOR plays critical roles in CSCs through stemness-related functions, and mTOR inhibition significantly leads to sensitization of CSCs (26). However, the potential of combinatorial treatment using PI3K/Akt/mTOR inhibitors and Sorafenib on LCSC population remains unclear. Therefore, two different sequential treatment strategies were followed: treatment of cells with strategy 1; Sorafenib or Doxorubicin before either mTOR inhibitor Rapamycin or PI3K inhibitor LY294002 or DAPT, and strategy 2; treatment of cells with Rapamycin or DAPT before Sorafenib. The first strategy failed to inhibit enrichment of LCSCs and even enhanced this process (Supplementary Fig. S5). However, the second strategy decreased the CD133⁺/EpCAM⁺ cells significantly in both Huh7 and Hep3B cells (Fig. 1B) and resulted in significantly smaller and lower number of spheres in cells treated with Rapamycin prior to Sorafenib (Fig. 1C). Consequently, strategy 2 was promising for the inhibition of LCSCs' enrichment compared with Sorafenib alone.

Gene expression and pathway analysis indicated IL8 responsible for LCSC enrichment under chemotherapeutic stress

In order to investigate the genes altered in cancer pathways and stemness-related molecular mechanisms in the presence of Sorafenib, Rapamycin, and DAPT, "PanCancer pathways" gene expression panel (770 genes) was analyzed with nCounter Technology. Differentially expressed gene (DEG) analysis revealed that upon Rapamycin or DAPT treatment, stemness pathway genes (*WNT* and *NOTCH*) were downregulated (Fig. 2A), whereas Sorafenib treatment caused upregulation of *JAG1* which encodes for Jagged-1, a Notch receptor ligand involved in cancer development and angiogenesis including HCC (ref. 27; Supplementary Fig. S6 and Supplementary DEG). When the top 15 DEGs were clustered with K-means-3 approach, the grouping of drug treatments was in correlation with our data given in Fig. 3 with regard to LCSC enrichment. In addition, expression of *FLNA* (Filamin A), *FLNC* genes (potential markers for the advanced HCC) were upregulated upon Sorafenib treatment (Fig. 2B; ref. 28).

DEG data were then used to perform "Score Flow" gene enrichment tool using Cytoscape software (enrichment strategy described in detail in Supplementary Fig. S7A; ref. 29) in order to evaluate the activity of cancer signaling pathways. *IL8* gene gained significantly enriched scores in Sorafenib-treated cells compared with DAPT or Rapamycin treatment (Fig. 2C). Parallel with the score flow analysis, when top 15 DEGs were clustered, *IL8* expression was strongly upregulated (~5-fold, log₂) upon Sorafenib treatment. In addition, Rapamycin treatment before

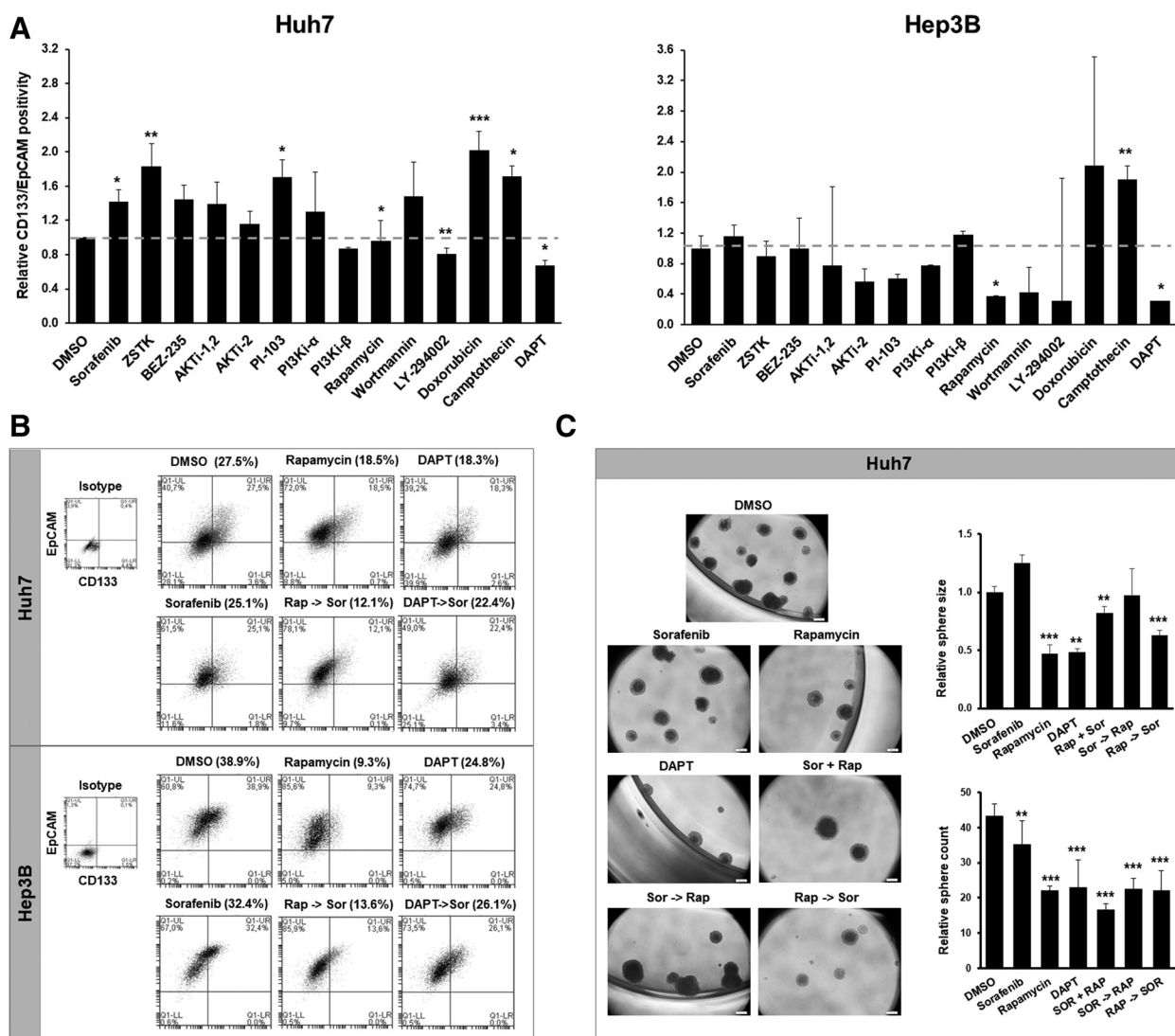


Figure 1.

Effects of small-molecule inhibitors on LCSC population from Huh7 and Hep3B cells. **A**, Bar graphs represent relative CD133/EpcAM positivity with respect to DMSO control group (red line: threshold). Experiments were done in 4 biological replicates at different times. DNA intercalators (Camptothecin and Doxorubicin) and Notch inhibitor, DAPT, were used as controls in this study. **B**, Representative flow cytometry results (top right plot) indicating positivity of CD133/EpcAM population after 72 hours of treatment with OMIC values of inhibitors versus control vehicle (DMSO). Cells that survived each treatment were collected and stained fluorescently by anti-CD133-biotin, anti-biotin-PE, and EpcAM-FITC antibodies. x axis indicates CD133 positivity, and y axis indicates EpcAM positivity. Lower-left quadrant, CD133⁻/EpcAM⁻; upper-left quadrant, CD133⁻/EpcAM⁺; lower-right quadrant, CD133⁺/EpcAM⁻; upper-right quadrant, CD133⁺/EpcAM⁺. Each treatment was compared with its corresponding DMSO control to define the changes in percentage of double-positive population. DAPT was used as positive control for CSC inhibition. **C**, Microscopy images represent spheres formed after 6 days by Huh7 cells treated with either a single inhibitor (OMIC values for 72 hours) or in combination [at the same time (Sor+Rap) or sequentially (Rap → Sor or Sor → Rap)] and inoculated into ultralow attachment plates in sphere formation media to be incubated in 37°C in a humidified incubator under 5% CO₂ until sphere formation was observed. Bar graphs represent sphere size and sphere count at day 6 for each treatment relative to DMSO-treated group.

Sorafenib resulted in the suppression of *IL8* along with *FLNA* and *FLNC* upregulation triggered by Sorafenib (Fig. 2B). Furthermore, clustering of the DEG data with the combination treatments supported our results with LCSC enrichment (Fig. 2B). Once the cells were treated with Rapamycin, DAPT, or Rapamycin and then Sorafenib, the expression of the above-mentioned genes was found to be regulated inversely. Altogether, DEG and score flow analysis results emphasized the potential of *IL8* as a target in the inhibition of LCSC enrichment.

IL8 expression is correlated with LCSC enrichment

In order to characterize the association of *IL8* with LCSC enrichment features, we carried out functional assays in the presence of the inhibitors. Initial confirmation of nCounter DEG data was done with qRT-PCR experiment. *NANOG* expression was in parallel with *IL8* expression in Huh7 cells and further decreased upon Rapamycin treatment (Fig. 3A). We then assessed the autocrine secretion of *IL8* with ELISA from tissue culture supernatants. *IL8* protein levels increased approximately 2-fold upon

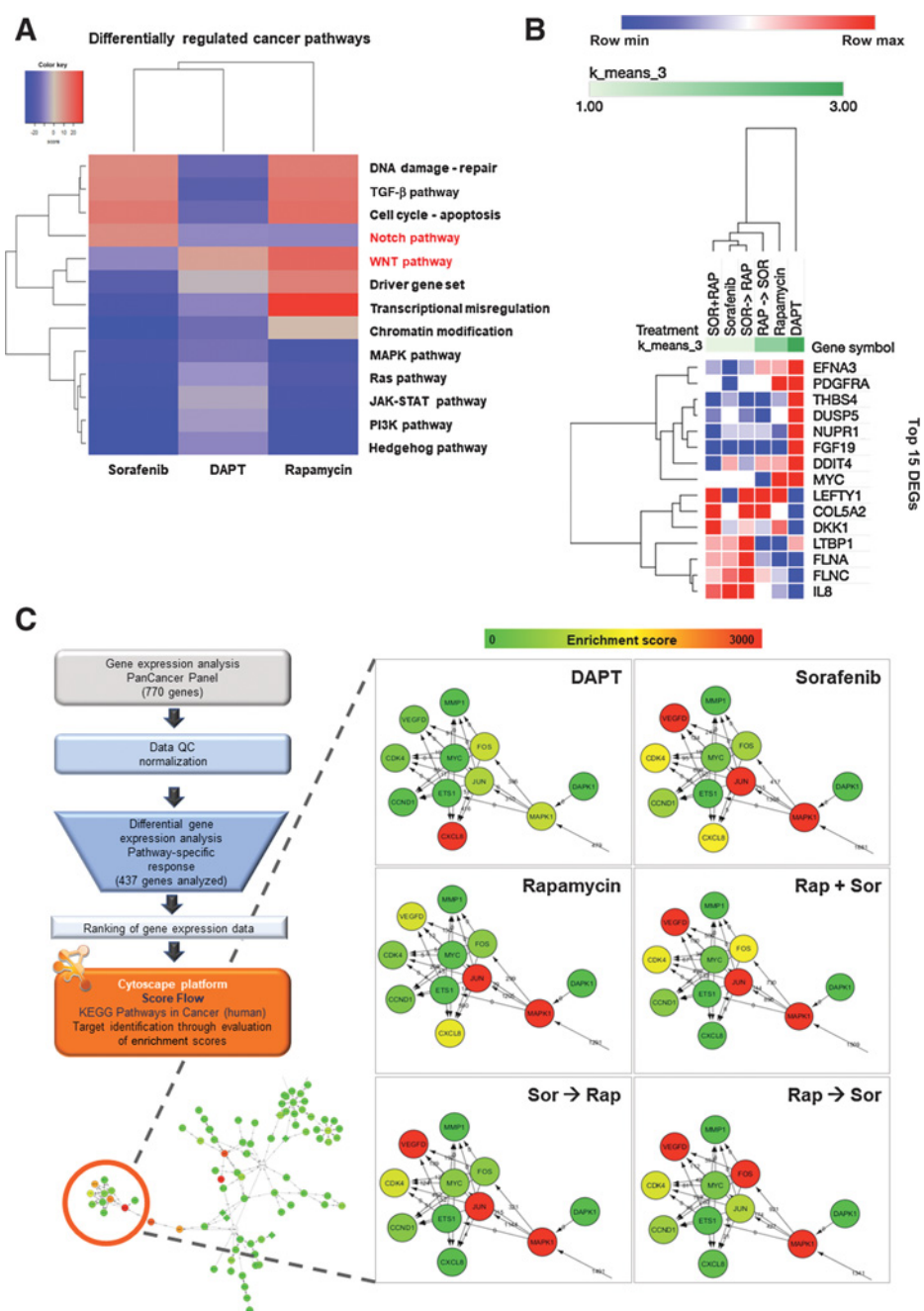
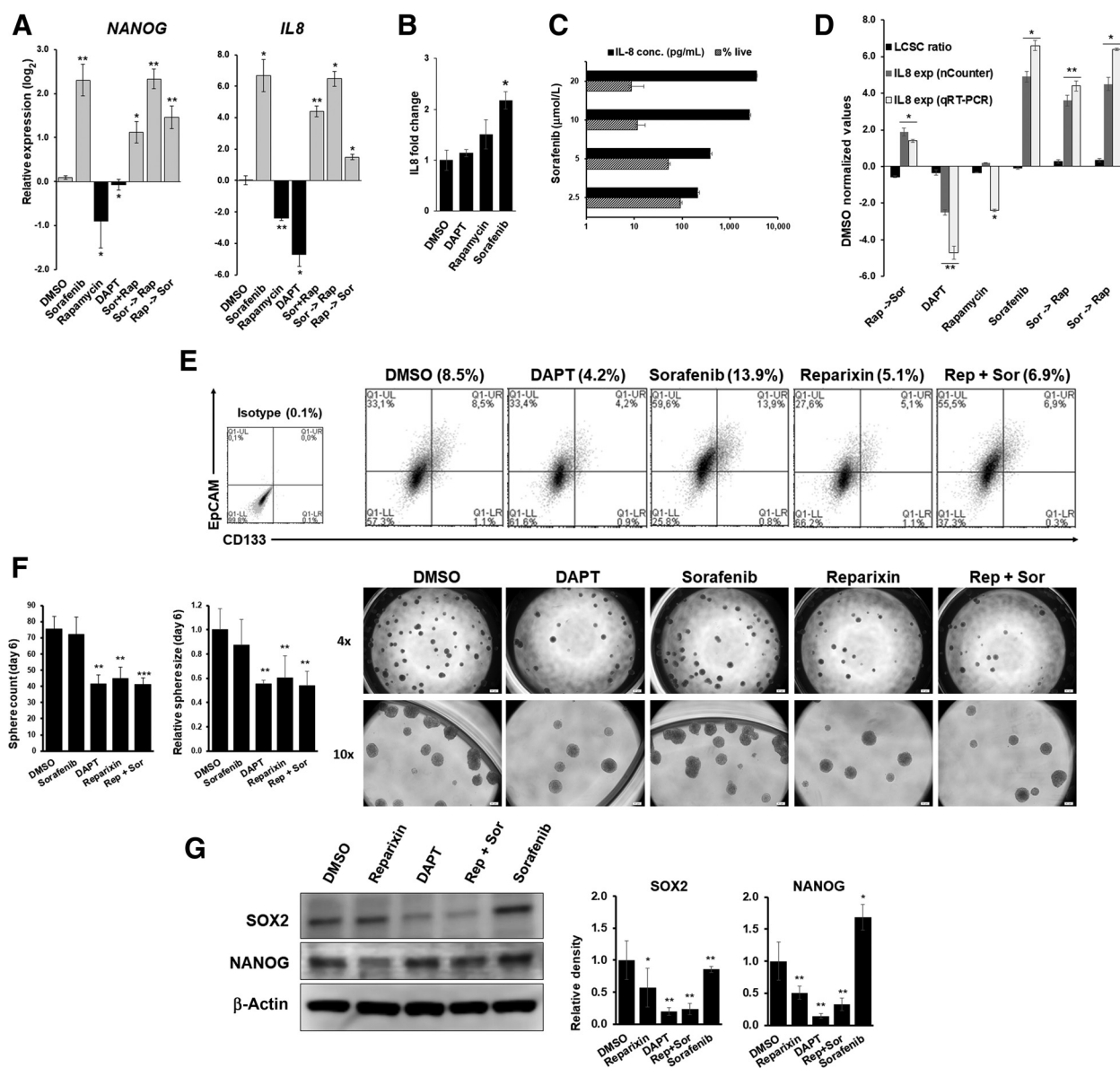


Figure 2.

Gene expression and score flow analysis of Huh7 cells treated with selected inhibitors and combination strategies. **A**, Heatmap representing the clustering of three different treatment groups (Sorafenib, DAPT, and Rapamycin) with respect to DEGs involved in different cancer pathways created by Advanced Analysis plug-in of Nanostring nSolver pathway enrichment analysis software. **B**, Heatmap and clustering analysis created with Morpheus, <https://software.broadinstitute.org/morpheus>, demonstrating the top 15 of the most significant DEGs in PanCancer pathways panel of Nanostring nCounter Technology with reference to DMSO control group. **C**, Pathway scoring results using differential gene expression data obtained from Nanostring nCounter platform. Flow chart of steps followed to adapt the differential gene expression data into our pathway scoring algorithm using Cytoscape platform and KEGG Pathways in Cancer (Homo sapiens) pathway. Initially, expression analysis of 770 genes involved in PanCancer pathway panel was done using the Nanostring nCounter technology and the analysis software available. After quality control and normalization of the expression data, advanced analysis software was used to obtain DEG in each group relative to DMSO. Among 770 genes, 437 were able to be statistically computable. Then, differential expression results of each treatment group were converted into ranked lists which include gene name, entrez gene id, and ranked DE value of each gene (as explained in the methods part), and loaded into Cytoscape 3.5 platform where "Score Flow" algorithm plug-in was run integrated with "Pathways in cancer (human)" KEGG pathway. The enrichment scores obtained were represented with a color scale where scores increase as the color shifts from green to red. Pathway scoring results of *CXCL8* (*IL8*) and the surrounding effectors were shown for each treatment group.

**Figure 3.**

IL8 expression is correlated with LCSC enrichment, and its inhibition sensitizes Huh7 cells to Sorafenib treatment. **A**, Bar graph demonstrating relative expression of *NANOG* and *IL8* obtained by qRT-PCR. **B**, IL-8 ELISA results showing secretion of IL8 in pg/mL from Huh7 cells treated with DAPT, Rapamycin, Sorafenib, or DMSO for 72 hours (OMIC values). Each treatment was performed in triplicates, and the results were normalized with respect to the percentage of viable cells after treatment. **C**, Bar graph shows secreted IL8 levels from Huh7 cells treated with different concentration of Sorafenib for 72 hours, with respect to percent live cells determined by SRB assay. **D**, Graph representing the correlation of *IL8* expression (both Nanostring and qRT-PCR) with CD133⁺/EpCAM⁺ population ratio in Huh7 cells. **E**, Flow cytometry analysis of Huh7 cells treated with OMIC values of indicated inhibitors for 72 hours. Table summarizing the % LCSC positivity for each treatment group. **F**, Representative 4x and 10x microscopic images of spheres formed by Huh7 cells after 72 hours of treatment with OMIC values of indicated inhibitors and bar graphs comparing the number of spheres for each treatment group and sphere size relative to DMSO control. **G**, Western blot analysis of whole lysate extracted from spheres of each treatment group. Representative images and bar graphs show protein levels of SOX2 and NANOG. β -Actin was used as loading control, and relative intensity values for both proteins were obtained using LI-COR Image Studio software.

treatment with Sorafenib and did not change significantly upon DAPT or Rapamycin treatment (Fig. 3B). Time- and dose-dependent ELISA experiments showed that, as the cell viability decreases upon Sorafenib treatment, IL8 concentrations increase (Fig. 3C; Supplementary Fig. S8). When we analyzed and compared the data in the presence of the inhibitors and their combinations from Fig. 1A in terms of LCSC ratio with *IL8* expression

originated from two different sources (direct hybridization with nCounter platform and qRT-PCR), there was a strong correlation between the ratio of LCSCs and the expression of *IL8*. As the LCSC population was enriched, the expression of *IL8* gene increased (Fig. 3D; Supplementary Fig. S9). As opposed to Sorafenib alone, Rapamycin treatment before Sorafenib prevented *IL8* gene expression upregulation, hence impeded the stemness switch of HCC

cells. *IL8* has been widely studied in many cancers including breast (30), lung (31), pancreatic (32), colorectal (33), and HCC (34), but not yet been associated with drug-resistant CSC-like properties under drug stress in HCC.

IL8 signaling inhibition or *IL8* silencing reduces stemness-related properties of Huh7 cells

Our results have led us to concentrate on the possibility that HCC cells could be sensitized to Sorafenib treatment through blockade of *IL8* signaling as we observed with the effect of Rapamycin. Reparixin (ref. 35; Cayman Chemical), *IL8* receptor inhibitor (IC_{50} : 50 μ mol/L), was used to inhibit *IL8* signaling in Huh7 and Hep3B cells. Reparixin alone and in combination with Sorafenib resulted in significant reduction in positivity of LCSC markers (Fig. 3E), as well as their capacity to form spheres (Fig. 3F). In addition, both NANOG and SOX2 protein levels were reduced in spheres formed by Huh7 cells treated with DAPT and Reparixin, compared with Sorafenib treatment. Moreover, the combination of Sorafenib and Reparixin resulted in lower levels of SOX2 and NANOG proteins (Fig. 3G).

Knockdown experiments were performed using three different siRNAs targeting *IL8* gene. Hs_IL8_6 FlexiTube siRNA was selected for further experiments due to its effective knockdown of *IL8* in Huh7 cells (Supplementary Fig. S10). siRNA treatment lead to reduced mRNA expression levels of *IL8* as well as NANOG after 48 hours (Fig. 4A). Autocrine secretion of *IL8* also decreased with respect to untreated or negative siRNA-treated Huh7 cells (Fig. 4B). CD133/EpCAM-positive population as well as the sphere formation capacity of Huh7 cells decreased significantly 72 hours after siRNA transfection (Fig. 4C). Simultaneously, the expression of epithelial marker E-cadherin and stemness marker SOX2 decreased significantly, indicating that knockdown of *IL8* increases both epithelial features of Huh7 cells and reduces stemness-related protein expression (Fig. 4D).

Moreover, the effects of *IL8* silencing on the sensitivity of cells to Sorafenib were investigated using an RT-CES. siRNA-transfected cells grew more slowly and were more sensitive to Sorafenib compared with untransfected controls, such that 10 μ mol/L Sorafenib resulted in twice the amount of growth inhibition in these cells (Fig. 4E). We concluded that both inhibition of *IL8* signaling as well as knockdown of *IL8* sensitized HCC cells toward treatment and reduced LCSC population in HCC cells.

Regorafenib induces upregulation of interleukins associated with stemness

We also evaluated LCSC enrichment in parallel with *IL8* expression on Huh7 cells in the presence of Regorafenib (another multikinase inhibitor approved for advanced HCC treatment, IC_{50} 1.5 μ mol/L; Selleck chemicals). Regorafenib enriched LCSC population (Fig. 5A) and upregulated not only *IL8*, but also other stemness-promoting interleukins such as *IL11* and *IL1 β* , as well as *STAT* expression (Fig. 5B; Supplementary Fig. S6B). Moreover, Sorafenib and Regorafenib treatment resulted in denser and larger spheres, whereas *IL8* signaling inhibition with Reparixin or DAPT treatment inhibited the number and the size of the spheres with respect to DMSO control (Fig. 5C). Furthermore, with the *Score Flow* algorithm applied to the DEG results of Regorafenib-treated cells, MAPK and PI3K gene expressions were significantly enriched

(Fig. 5D). Altogether, Regorafenib and Sorafenib lead to the enrichment of CD133⁺/EpCAM⁺ population and upregulate cytokines associated with stemness switch which can be prevented with adjuvant therapies.

Discussion

Studies focusing on the mechanisms underlying the heterogeneity of HCC and the acquired resistance to chemotherapeutics reported that the activation of compensatory pathways such as PI3K/Akt/mTOR, JAK-STAT signaling, and the existence of LCSC population are involved in drug resistance (36). In this study, we initially characterized CD133 and EpCAM marker positivity as LCSC markers in Huh7 and Hep3B cells and further validated with sphere formation and expression of NANOG and OCT4 as reported previously (Supplementary Fig. S2; ref. 37). Literature has also defined the association between PI3K/Akt/mTOR pathway and LCSC markers CD133 and EpCAM through analysis of tumor and nontumor tissues from HCC patients and found that p-Akt and p-mTOR expressions were positively correlated with stemness marker expression (37). Although Sorafenib and other small-molecule kinase inhibitors targeting PI3K/Akt or Ras/Raf pathways are widely studied for their anticancer activity, it is a great concern that their efficacy is unpredictable in HCC patients due to high-level tumor heterogeneity. Because Sorafenib inhibits Raf/(MAPK) signaling but activates PI3K/Akt pathway (ref. 38; Supplementary Fig. S2), it is suggested that combinations targeting PI3K/Akt/mTOR or Ras/MAK pathways could be promising in ensuring better clinical outcomes. PKI-587, an inhibitor of PI3K/Akt/mTOR pathway together with Sorafenib, is reported to be advantageous in HCC (39). However, a recently completed phase II clinical trial (40) which compares everolimus (PI3K/Akt/mTOR pathway inhibitor) combined with Sorafenib and a phase III trial of Sorafenib and erlotinib (EGFR inhibitor; ref. 41) showed no improved survival rates compared with Sorafenib alone (42). Given the fact that not all PI3K/Akt/mTOR pathway inhibitors exhibit promising effect on HCC, in this study a group of small-molecule inhibitors targeting PI3K/Akt/mTOR pathway, Sorafenib, and clinically used DNA intercalators (Camptothecin, Doxorubicin) were investigated for their efficacy against LCSCs. As expected, and in parallel with the literature, each inhibitor was found to have differential action on LCSCs where Sorafenib and DNA intercalators and PI3K/Akt pathway inhibitors ZSTK and NVP-BEZ235 enriched LCSC population, whereas Rapamycin and LY294002 decreased this population significantly (Fig. 1). The potent inhibitors against LCSCs were then further tested in combination with Sorafenib to propose a treatment strategy that would inhibit LCSC enrichment and sensitize cells to Sorafenib. Sequential treatment with Rapamycin prior to Sorafenib resulted in reduced levels of LCSCs (Fig. 1). When the order of inhibitors was changed, LCSCs were likely to enrich even more compared with Sorafenib treatment alone (Supplementary Fig. S5). We concluded that pretreatment of cells with Rapamycin regulates stemness-related factors and sensitizes LCSCs toward sorafenib. The potential of mTOR pathway inhibitors has already been shown in stemness-related pathways indicating that these inhibitors act on the proliferation of CSCs and non-CSCs in Huh7 cells equally (43).

To understand the alterations in the expression patterns of cancer pathway-related genes and to identify novel molecular targets that could have a significant role in survival mechanisms

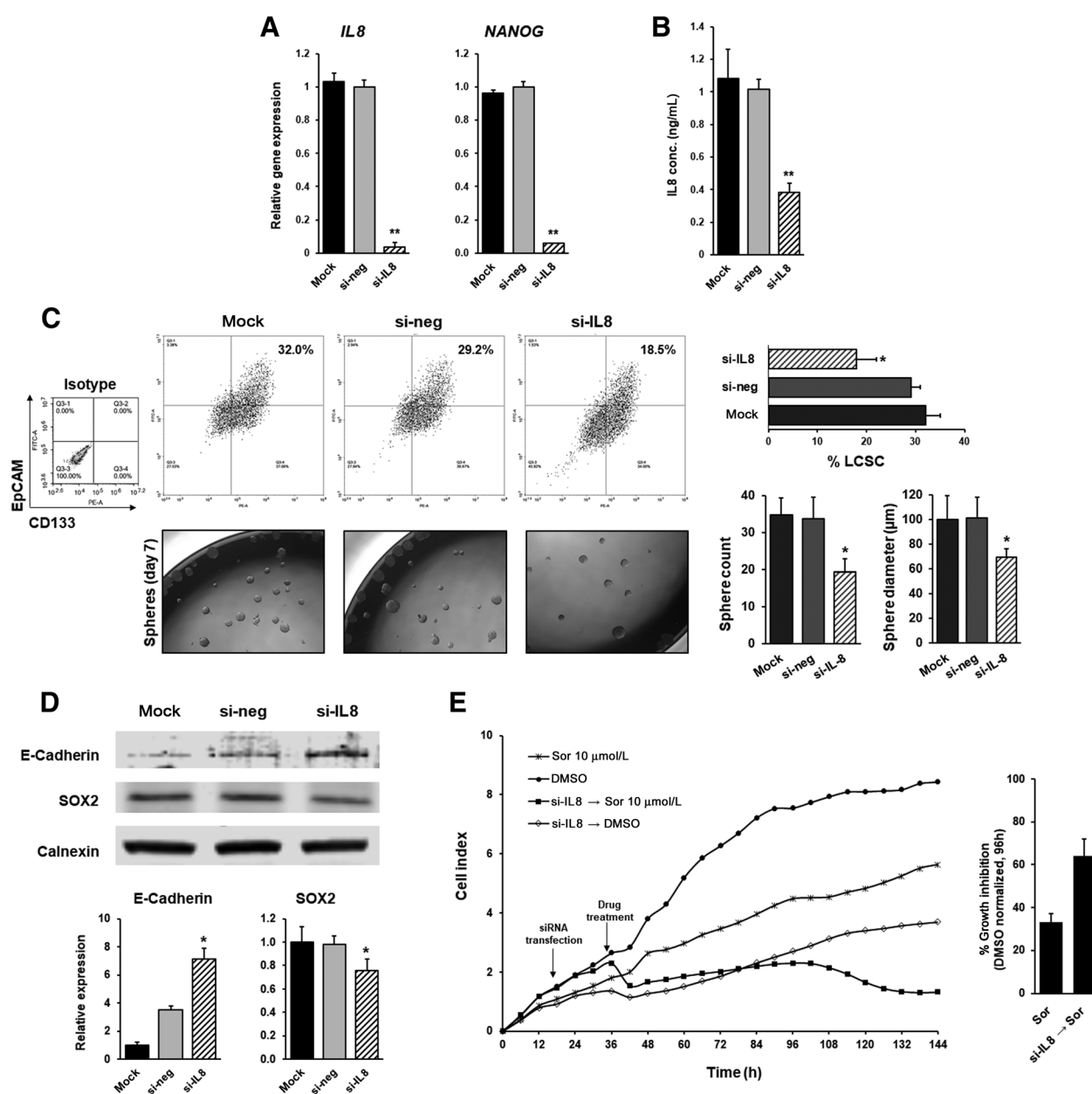


Figure 4.

Knockdown of *IL8* adversely affects stemness and sensitizes Huh7 cells to Sorafenib. **A**, Bar graphs represent relative gene expression (*IL8* or *NANOG*) in Huh7 cells treated with si-*IL8* (50 nmol/L), negative control siRNA, or remained untransfected (mock) for 48 hours. **B**, Bar graph shows secretion of IL8 from Huh7 cells after 48 hours determined by ELISA experiments. **C**, Representative images of flow cytometry analysis of CD133⁺/EPCAM⁺ cells (top row) and sphere formation assay results (bottom row) of Huh7 cells after treatment with siRNA. Bar graphs represent the number of spheres for each treatment group and sphere size relative to mock and neg-siRNA control. **D**, Representative images and bar graphs show protein levels of E-cadherin and SOX2 with respect to Calnexin (loading control) in siRNA-treated Huh7 cells. Relative signal intensity values for both proteins were obtained using LI-COR Image Studio software. **E**, Line graph obtained from RT-CES SP system shows growth of Huh7 cells treated with Sorafenib only or after *IL8* knockdown. Percent cell inhibition values are represented in bar graph for each group using cell index values that correspond to DMSO-normalized 96-hour treatment.

of LCSCs, a panel consisting of 770 genes were studied and analyzed using nCounter technology based on direct hybridization of cellular RNA (Fig. 2). Upon DAPT or Rapamycin treatment, genes related with Notch pathway were downregulated as expected. Differential expression analysis revealed that expression of Ras and MAPK pathway-related

genes (*PDGFRA*, *EFNA1*, *EFNA3*, *VEGFA*, and *RASA4*) were downregulated, whereas genes belonging to Wnt and Notch pathway (*DKK1* and *JAG1*) were upregulated upon treatment with Sorafenib. The differential expression data in the presence of selected inhibitors were further analyzed with the score flow algorithm (Cytoscape gene prioritization application) to

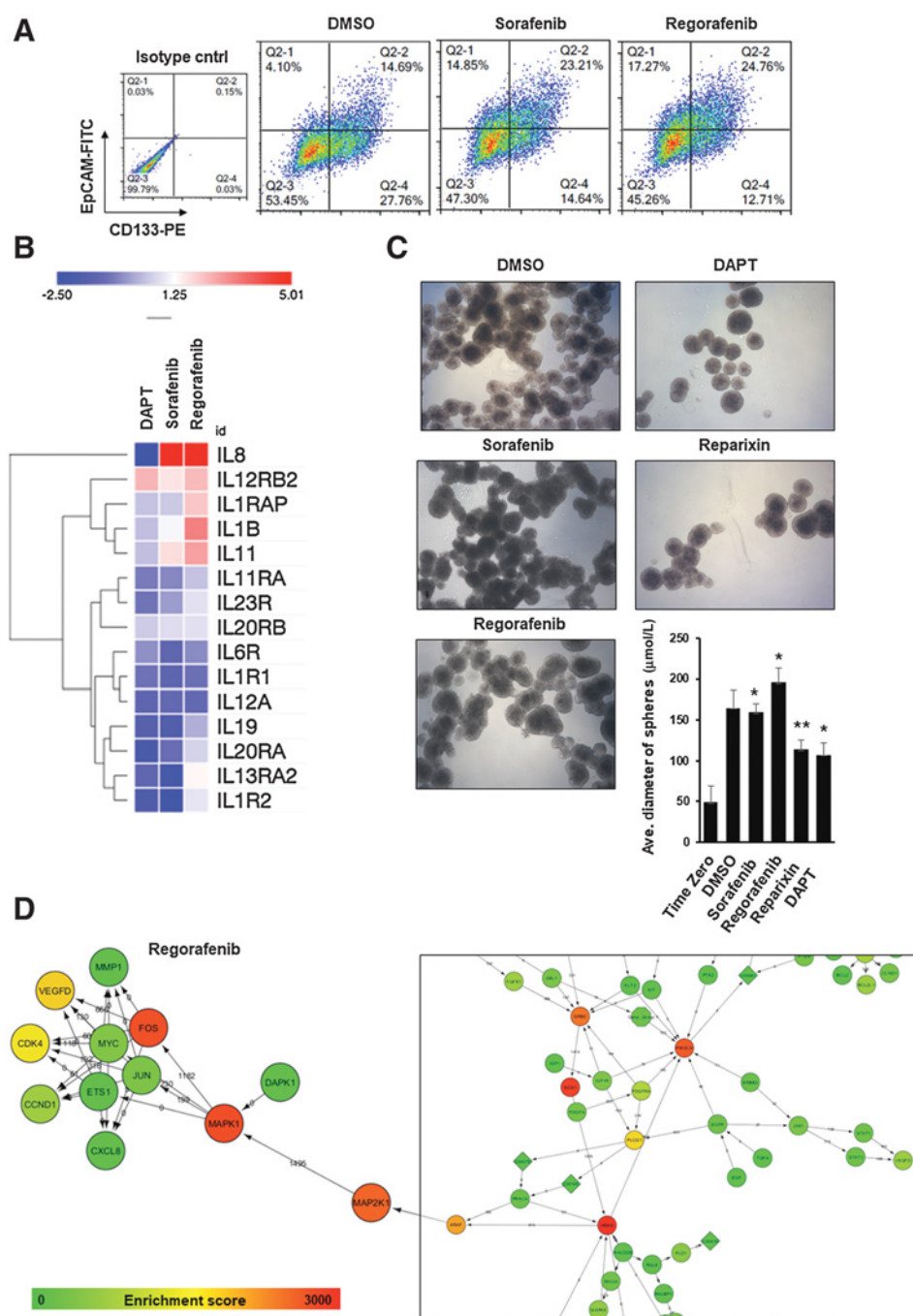


Figure 5. Effects of Regorafenib on LCSC enrichment and expression of *IL8*. **A**, Flow cytometry analysis demonstrating the changes in the percentage of CD133⁺/EpCAM⁺ populations upon treatment with Sorafenib and Regorafenib (OMIC concentration for 72 hours). **B**, Heatmap representing the differential expression of various interleukins included in PanCancer pathways panel, in DAPT-, Sorafenib-, and Regorafenib-treated Huh7 cells with reference to DMSO control group. **C**, Treatment of spheres (formed at day 5) from Huh7 cells with Regorafenib, Sorafenib, Reparixin, and DAPT for 72 hours. Changes in the sphere size are demonstrated and quantified as shown in the bar graph. **D**, Cytoscape score flow analysis of the DEG data of Regorafenib-treated Huh7 cells demonstrating the genes with enriched scores (red).

evaluate the activity of KEGG cancer signaling pathway (Fig. 2C). This gene prioritization application does not only enrich the DEGs but also depends on the network topology. The score flow algorithm, using the expression data, calculates weights for the protein nodes considering protein-protein interaction edge connectivity information such as feedbacks and loops within the pathway. This method allowed us to single out *IL8* as a significant differential target during Sorafenib, DAPT, Rapamycin, and combination treatments when compared with simple DEG analysis. Autocrine *IL8* secretion

by liver cancer cells was previously reported, along with its possible role in tumor growth and angiogenesis, suggesting *IL8* as a potential target for liver cancer therapy (44). However, there is not any study indicating the involvement of *IL8* in drug resistance-related liver cancer stemness (34).

Tumor cells produce factors to attract and regulate a variety of cell types in their microenvironment. The inflammatory cytokines *IL1β*, *IL6*, and *IL8* play essential roles in regulating the interaction between LCSCs and their microenvironment by activating Stat3/NF-κB pathways in both tumor and stromal cells. Due to the activation of these

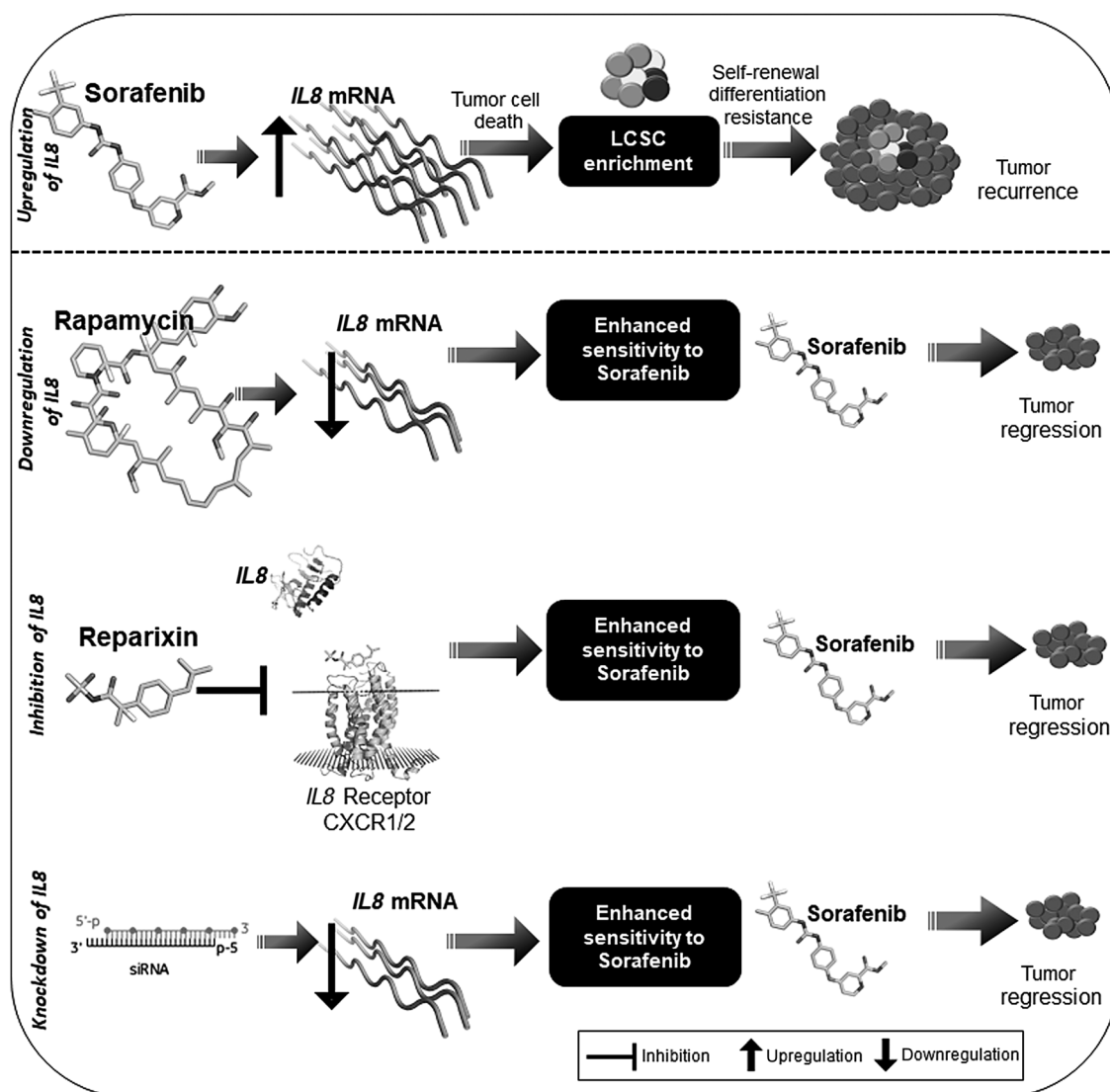


Figure 6.

Regulation of stemness-related factors in the presence of Sorafenib and Regorafenib leads to LCSC enrichment. Sorafenib and Regorafenib treatment results in upregulation of *IL8*, which is associated with the enrichment of LCSCs. Rapamycin treatment before Sorafenib, targeting the IL8 signaling by Reparixin, or knockdown of *IL8* reduces Sorafenib-dependent LCSC enrichment and sensitizes HCC cells to Sorafenib.

pathways, further cytokine production causes positive feedback loops that stimulate self-renewal of LCSC (10). In this study, differential expression of *IL8* under various drug treatments draws our attention because IL8 signaling has been studied in other cancers, especially in breast cancer, and its knockout resulted in poor survival of BCSCs (30). In fact, it has been reported previously that *IL8* levels increase during progression of HCC and play role in development of distant metastasis (45). Another study has described that *IL8* plays an important role in driving HCC tumor growth, self-renewal, and angiogenesis in CD133⁺ liver cancer cells (34). In our study, treatment of cells with Rapamycin prior to Sorafenib prevented the upregulation of *IL8* unlike other combination strategies, which further suggested that Rapamycin could be inducing cellular events that do not allow *IL8* expression to elevate, yet triggers a mechanism which inhibits survival of LCSCs. *IL8* expression was signifi-

cantly correlated with *NANOG* expression and LCSC ratio in Huh7 cells (Fig. 3A). In fact, inhibition of IL8 through treatment with its receptor inhibitor Reparixin resulted in the reduction of CD133⁺/EpCAM⁺ population, their sphere formation capacity, and the levels of stemness-related proteins (Fig. 3E–G). Comparably, identical results were obtained from knockdown experiments of *IL8* gene in Huh7 cells (Fig. 4C and D), and sensitivity of Huh7 cells to Sorafenib was increased when cells were transfected with *IL8* siRNA beforehand (Fig. 4E). Altogether, both IL8 signaling inhibition and *IL8* knockdown enhance sensitivity toward Sorafenib treatment in HCC cells and display inhibitory effects on survival of stem cell-like cancer cells, correlated with the data represented in previous studies on other cancer types (30, 31, 46, 47).

Apart from Sorafenib, a recently FDA-approved multikinase inhibitor Regorafenib also enriched LCSC population and

upregulated several inflammatory cytokines (*IL8*, *IL11*, and *IL1 β* ; Fig. 5). The upregulation and secretion of these inflammatory cytokines from cancer cells were associated with the enrichment of side populations, which further emphasizes the effect of autocrine signaling on LCSCs and their regulation of survival under chemotherapeutic stress.

In summary (Fig. 6), the data represented herein elucidate the mechanisms associated with the survival of LCSC population under drug stress. We provide a better understanding of alterations in distribution of stem/nonstem cells with different Akt/mTOR pathway inhibitors along with clinically administered chemotherapeutic agents Sorafenib and Regorafenib. Finally, expression and functional analysis of the cellular pathways under drug stress allowed us to identify Rapamycin as one of the drugs capable of suppressing the overexpression of inflammatory cytokines, particularly IL8 pathway as a target involved in the regulation of LCSC survival. The data address the necessity for new approaches against HCC in clinics because Rapamycin is already in use for various liver diseases and Reparixin is exploited in clinical trials for other cancers.

Disclosure of Potential Conflicts of Interest

No potential conflicts of interest were disclosed.

References

- Stewart BW, Wild CP, editors. World cancer report. Lyon, France: International Agency for Research on Cancer, World Health Organization; 2014, p. 630.
- Xu J. Trends in liver cancer mortality among adults aged 25 and over in the United States, 2000-2016. NCHS Data Brief 2018;1-8.
- European Association for the Study of the Liver. Electronic address: easloffice@easloffice.eu; European Association for the Study of the Liver. EASL clinical practice guidelines: management of hepatocellular carcinoma. J Hepatol 2018;69:182-236.
- Baffy G, Brunt EM, Caldwell SH. Hepatocellular carcinoma in non-alcoholic fatty liver disease: an emerging menace. J Hepatol 2012;56:1384-91.
- Yamashita T, Wang XW. Cancer stem cells in the development of liver cancer. J Clin Invest 2013;123:1911-8.
- Zhai B, Sun XY. Mechanisms of resistance to sorafenib and the corresponding strategies in hepatocellular carcinoma. World J Hepatol 2013;5:345-52.
- Whittaker S, Marais R, Zhu AX. The role of signaling pathways in the development and treatment of hepatocellular carcinoma. Oncogene 2010;29:4989-5005.
- Wang L, Wang WL, Zhang Y, Guo SP, Zhang J, Li QL. Epigenetic and genetic alterations of PTEN in hepatocellular carcinoma. Hepatol Res 2007;37:389-96.
- Zhu YJ, Zheng B, Wang HY, Chen L. New knowledge of the mechanisms of sorafenib resistance in liver cancer. Acta Pharmacol Sin 2017;38:614-22.
- Korkaya H, Liu S, Wicha MS. Regulation of cancer stem cells by cytokine networks: attacking cancer's inflammatory roots. Clin Cancer Res 2011;17:6125-9.
- Park SY, Han J, Kim JB, Yang MG, Kim YJ, Lim HJ, et al. Interleukin-8 is related to poor chemotherapeutic response and tumorigenicity in hepatocellular carcinoma. Eur J Cancer 2014;50:341-50.
- Oefinger PE, Bronson DL, Dreesman GR. Induction of hepatitis B surface antigen in human hepatoma-derived cell lines. J Gen Virol 1981;53:105-13.
- Kahraman DC, Hanquet G, Jeanmart L, Lanners S, Sramel P, Bohac A, et al. Quinoides and VEGFR2 TKIs influence the fate of hepatocellular carcinoma and its cancer stem cells. Medchemcomm 2017;8:81-7.
- Yamashita T, Kaneko S. Orchestration of hepatocellular carcinoma development by diverse liver cancer stem cells. J Gastroenterol 2014;49:1105-10.
- Kepler JA, Wani MC, McNaull JN, Wall ME, Levine SG. Plant antitumor agents. IV. An approach toward the synthesis of camptothecin. J Org Chem 1969;34:3853-8.
- Di Marco A, Gaetani M, Scarpinato B. Adriamycin (NSC-123,127): a new antibiotic with antitumor activity. Cancer Chemother Rep 1969;53:33-7.
- Yaguchi S, Fukui Y, Koshimizu I, Yoshimi H, Matsuno T, Gouda H, et al. Antitumor activity of ZSTK474, a new phosphatidylinositol 3-kinase inhibitor. J Natl Cancer Inst 2006;98:545-56.
- Maira SM, Stauffer F, Brueggen J, Furet P, Schnell C, Fritsch C, et al. Identification and characterization of NVP-BEZ235, a new orally available dual phosphatidylinositol 3-kinase/mammalian target of rapamycin inhibitor with potent in vivo antitumor activity. Mol Cancer Ther 2008;7:1851-63.
- Lindsley CW, Zhao Z, Leister WH, Robinson RG, Barnett SF, Defeo-Jones D, et al. Allosteric Akt (PKB) inhibitors: discovery and SAR of isozyme selective inhibitors. Bioorg Med Chem Lett 2005;15:761-4.
- Zhao Z, Robinson RG, Barnett SF, Defeo-Jones D, Jones RE, Hartman GD, et al. Development of potent, allosteric dual Akt1 and Akt2 inhibitors with improved physical properties and cell activity. Bioorg Med Chem Lett 2008;18:49-53.
- Hayakawa M, Kawaguchi K, Kaizawa H, Koizumi T, Ohishi T, Yamano M, et al. Synthesis and biological evaluation of sulfonylethylhydrazide-substituted imidazo[1,2-a]pyridines as novel PI3 kinase p110alpha inhibitors. Bioorg Med Chem 2007;15:5837-44.
- Mateo J, Ganji G, Lemech C, Burris HA, Han SW, Swales K, et al. A first-time-in-human study of GSK2636771, a phosphoinositide 3 kinase beta-selective inhibitor, in patients with advanced solid tumors. Clin Cancer Res 2017;23:5981-92.
- Graziani EI. Recent advances in the chemistry, biosynthesis and pharmacology of rapamycin analogs. Nat Prod Rep 2009;26:602-9.
- Vlahos CJ, Matter WF, Hui KY, Brown RF. A specific inhibitor of phosphatidylinositol 3-kinase, 2-(4-morpholinyl)-8-phenyl-4H-1-benzopyran-4-one (LY294002). J Biol Chem 1994;269:5241-8.
- Kan T, Tominari Y, Rikimaru K, Morohashi Y, Natsugari H, Tomita T, et al. Parallel synthesis of DAPT derivatives and their gamma-secretase-inhibitory activity. Bioorg Med Chem Lett 2004;14:1983-5.
- Lai YH, Yu XP, Lin XH, He SY. Inhibition of mTOR sensitizes breast cancer stem cells to radiation-induced repression of self-renewal through the regulation of MnSOD and Akt. Int J Mol Med 2016;37:369-77.

Authors' Contributions

Conception and design: D.C. Kahraman, T. Kahraman, R. Cetin-Atalay
Development of methodology: D.C. Kahraman, T. Kahraman, R. Cetin-Atalay
Acquisition of data (provided animals, acquired and managed patients, provided facilities, etc.): D.C. Kahraman
Analysis and interpretation of data (e.g., statistical analysis, biostatistics, computational analysis): D.C. Kahraman, T. Kahraman, R. Cetin-Atalay
Writing, review, and/or revision of the manuscript: D.C. Kahraman, T. Kahraman, R. Cetin-Atalay
Administrative, technical, or material support (i.e., reporting or organizing data, constructing databases): R. Cetin-Atalay
Study supervision: R. Cetin-Atalay

Acknowledgments

The authors acknowledge the Turkish Ministry of Strategy and Budget grant (Ref: 2016K121540) and the Scientific and Technological Research Council of Turkey (TUBITAK) grant (Ref: 113S540) received by R. Cetin-Atalay. The authors would also like to thank Professor Dr. Ihsan Gursel for his valuable comments during this study.

The costs of publication of this article were defrayed in part by the payment of page charges. This article must therefore be hereby marked *advertisement* in accordance with 18 U.S.C. Section 1734 solely to indicate this fact.

Received February 1, 2019; revised March 1, 2019; accepted August 15, 2019; published first August 22, 2019.

27. Capaccione KM, Pine SR. The Notch signaling pathway as a mediator of tumor survival. *Carcinogenesis* 2013;34:1420–30.
28. Ai JZ, Huang HZ, Lv XY, Tang ZW, Chen MZ, Chen TL, et al. FLNA and PGK1 are two potential markers for progression in hepatocellular carcinoma. *Cell Physiol Biochem* 2011;27:207–16.
29. Isik Z, Ersahin T, Atalay V, Aykanat C, Cetin-Atalay R. A signal transduction score flow algorithm for cyclic cellular pathway analysis, which combines transcriptome and CHIP-seq data. *Mol Biosyst* 2012;8:3224–31.
30. Singh JK, Simoes BM, Howell SJ, Farnie G, Clarke RB. Recent advances reveal IL-8 signaling as a potential key to targeting breast cancer stem cells. *Breast Cancer Res* 2013;15.
31. Liu YN, Chang TH, Tsai MF, Wu SG, Tsai TH, Chen HY, et al. IL-8 confers resistance to EGFR inhibitors by inducing stem cell properties in lung cancer. *Oncotarget* 2015;6:10415–31.
32. Chen LY, Fan J, Chen H, Meng ZQ, Chen Z, Wang P, et al. The IL-8/CXCR1 axis is associated with cancer stem cell-like properties and correlates with clinical prognosis in human pancreatic cancer cases. *Sci Rep* 2014;4:5911.
33. Wang JC, Wang YN, Wang SC, Cai JY, Shi JQ, Sui X, et al. Bone marrow-derived mesenchymal stem cell-secreted IL-8 promotes the angiogenesis and growth of colorectal cancer. *Oncotarget* 2015;6:42825–37.
34. Tang KH, Ma S, Lee TK, Chan YP, Kwan PS, Tong CM, et al. CD133+ liver tumor-initiating cells promote tumor angiogenesis, growth, and self-renewal through neurotensin/interleukin-8/CXCL1 signaling. *Hepatology* 2012;55:807–20.
35. Moriconi A, Cesta MC, Cervellera MN, Aramini A, Coniglio S, Colagioia S, et al. Design of noncompetitive interleukin-8 inhibitors acting on CXCR1 and CXCR2. *J Med Chem* 2007;50:3984–4002.
36. Palmer DH. Sorafenib in advanced hepatocellular carcinoma. *New Engl J Med* 2008;359:2498.
37. Su RJ, Nan HC, Guo H, Ruan ZP, Jiang LL, Song YY, et al. Associations of components of PI3K/AKT/mTOR pathway with cancer stem cell markers and prognostic value of these biomarkers in hepatocellular carcinoma. *Hepatol Res* 2016;46:1380–91.
38. Wang CM, Cigliano A, Delogu S, Armbruster J, Dombrowski F, Evert M, et al. Functional crosstalk between AKT/mTOR and Ras/MAPK pathways in hepatocarcinogenesis implications for the treatment of human liver cancer. *Cell Cycle* 2013;12:1999–2010.
39. Gedaly R, Angulo P, Hundley J, Daily ME, Chen CG, Evers BM. PKI-587 and sorafenib targeting PI3K/AKT/mTOR and Ras/Raf/MAPK pathways synergistically inhibit HCC cell proliferation. *J Surg Res* 2012;176:542–8.
40. Koeberle D, Dufour JF, Demeter G, Li Q, Ribi K, Samaras P, et al. Sorafenib with or without everolimus in patients with advanced hepatocellular carcinoma (HCC): a randomized multicenter, multinational phase II trial (SAKK 77/08 and SASL 29). *Ann Oncol* 2016;27:856–61.
41. Zhu AX, Rosmorduc O, Evans TR, Ross PJ, Santoro A, Carrilho FJ, et al. SEARCH: a phase III, randomized, double-blind, placebo-controlled trial of sorafenib plus erlotinib in patients with advanced hepatocellular carcinoma. *J Clin Oncol* 2015;33:559–66.
42. Chen J, Jin RN, Zhao J, Liu JH, Ying HN, Yan H, et al. Potential molecular, cellular and microenvironmental mechanism of sorafenib resistance in hepatocellular carcinoma. *Cancer Lett* 2015;367:1–11.
43. Hayashi T, Yamashita T, Okada H, Oishi N, Sunagozaka H, Nio K, et al. A novel mTOR inhibitor, anthracimycin for the treatment of human hepatocellular carcinoma. *Anticancer Res* 2017;37:3397–403.
44. Miyamoto M, Shimizu Y, Okada K, Kashii Y, Higuchi K, Watanabe A. Effect of interleukin-8 on production of tumor-associated substances and autocrine growth of human liver and pancreatic cancer cells. *Cancer Immunol Immun* 1998;47:47–57.
45. Ren Y, Poon RTP, Tsui HT, Chen WH, Li Z, Lau CL, et al. Interleukin-8 serum levels in patients with hepatocellular carcinoma: correlations with clinicopathological features and prognosis. *Clin Cancer Res* 2003;9:5996–6001.
46. Singh JK, Simoes BM, Clarke RB, Bundred NJ. Targeting IL-8 signalling to inhibit breast cancer stem cell activity. *Expert Opin Ther Tar* 2013;17:1235–41.
47. Chen L, Fan J, Chen H, Meng Z, Chen Z, Wang P, et al. The IL-8/CXCR1 axis is associated with cancer stem cell-like properties and correlates with clinical prognosis in human pancreatic cancer cases. *Sci Rep* 2014;4:5911.

Molecular Cancer Therapeutics

Targeting PI3K/Akt/mTOR Pathway Identifies Differential Expression and Functional Role of IL8 in Liver Cancer Stem Cell Enrichment

Deniz Cansen Kahraman, Tamer Kahraman and Rengul Cetin-Atalay

Mol Cancer Ther 2019;18:2146-2157. Published OnlineFirst August 22, 2019.

Updated version Access the most recent version of this article at:
doi:[10.1158/1535-7163.MCT-19-0004](https://doi.org/10.1158/1535-7163.MCT-19-0004)

Supplementary Material Access the most recent supplemental material at:
<http://mct.aacrjournals.org/content/suppl/2019/08/22/1535-7163.MCT-19-0004.DC1>

Cited articles This article cites 44 articles, 7 of which you can access for free at:
<http://mct.aacrjournals.org/content/18/11/2146.full#ref-list-1>

E-mail alerts [Sign up to receive free email-alerts](#) related to this article or journal.

Reprints and Subscriptions To order reprints of this article or to subscribe to the journal, contact the AACR Publications Department at pubs@aacr.org.

Permissions To request permission to re-use all or part of this article, use this link
<http://mct.aacrjournals.org/content/18/11/2146>.
Click on "Request Permissions" which will take you to the Copyright Clearance Center's (CCC) Rightslink site.